Three-dimensional tracking of Cuvier's beaked whales' echolocation sounds using nested hydrophone arrays

Martin Gassmann,[a] Sean M. Wiggins, and John A. Hildebrand
Scripps Institution of Oceanography, 9500 Gilman Drive, La Jolla, California 92093-0205, USA

(Received 1 April 2015; revised 4 July 2015; accepted 13 July 2015; published online 28 October 2015)

Cuvier's beaked whales (*Ziphius cavirostris*) were tracked using two volumetric small-aperture (~1 m element spacing) hydrophone arrays, embedded into a large-aperture (~1 km element spacing) seafloor hydrophone array of five nodes. This array design can reduce the minimum number of nodes that are needed to record the arrival of a strongly directional echolocation sound from 5 to 2, while providing enough time-differences of arrivals for a three-dimensional localization without depending on any additional information such as multipath arrivals. To illustrate the capabilities of this technique, six encounters of up to three Cuvier's beaked whales were tracked over a two-month recording period within an area of 20 km^2 in the Southern California Bight. Encounter periods ranged from 11 min to 33 min. Cuvier's beaked whales were found to reduce the time interval between echolocation clicks while alternating between two inter-click-interval regimes during their descent towards the seafloor. Maximum peak-to-peak source levels of 179 and 224 dB re 1 μPa @ 1 m were estimated for buzz sounds and on-axis echolocation clicks (directivity index = 30 dB), respectively. Source energy spectra of the on-axis clicks show significant frequency components between 70 and 90 kHz, in addition to their typically noted FM upsweep at 40–60 kHz.
 [http://dx.doi.org/10.1121/1.4927417]

[WWA] Pages: 2483–2494

I. INTRODUCTION

Animal tracking can be used to study their migration, behavior, abundance, and responses to man-made influences. Current tracking methods for marine mammals include visual observations, attaching small tracking devices ("tags") to them, and passive acoustic monitoring that utilizes their emitted sounds. Visual tracking is difficult for deep-diving marine mammals, such as beaked whales, which are most often submerged below the sea surface. It is possible to attach tags to beaked whales, for example, short-term (~24 h) suction-cup archival tags to provide high-resolution depth profiles along with wide bandwidth recorded sound (Tyack *et al.*, 2006), but it is difficult to infer detailed horizontal movement patterns and their position relative to local seafloor depths from these data. In contrast, barb-attached satellite tags provide large-scale horizontal movement patterns for up to a several months, but the resolution of their movements is coarse, as satellite-based locations are estimated only several times per day when the whale is at the surface (Schorr *et al.*, 2014). Independent of the type of tag used, their attachment may alter the beaked whales' behavior and it is usually challenging to attach them, limiting the number of tagged individuals.

Passive acoustic tracking methods can be applied to toothed whales by localizing their repeatedly transmitted echolocation pulses with hydrophone arrays deployed near the sea surface. For example, three-dimensional tracking from a floating instrument platform has been demonstrated for killer whales that dive at shallow depths (Gassmann *et al.*, 2013), while for deep-diving beaked whales bearings were estimated from a towed hydrophone array (Yack *et al.*, 2013). Although ranging with a towed hydrophone is possible, certain conditions on the geometry between the beaked whale and the towed array are required and limit its ranging capabilities (Zimmer, 2013).

Another approach to track deep-diving toothed whales is to use bottom-mounted hydrophones. For example, three-dimensional tracking has been demonstrated for a sperm whale by utilizing the arrival times of direct paths, surface and bottom reflections from its intense echolocation sounds recorded on a single, moored hydrophone (Tiemann *et al.*, 2006). However, one of the limiting requirements of this multipath arrival technique is a seafloor that significantly varies horizontally around the hydrophone location. For tracking deep-diving sperm whales over any bathymetry, their echolocations sounds, although narrow beam, are intense enough in directions other than the main beam to be received on conventional seafloor arrays with the receivers spaced several kilometers apart. By computing a sufficient number of time-difference of arrivals (TDOAs) between receivers for each echolocation sound, three-dimensional trajectories of sperm whales can be reconstructed, e.g., Nosal and Frazer (2007). In contrast to sperm whales, it is more challenging to receive echolocation sounds of beaked whales on a sufficient number of kilometer-spaced receivers for three-dimensional tracking due to greater frequency absorption at their dominant frequencies (>10 dB/km) and lower source levels (Zimmer *et al.*, 2005). To aid three-dimensional tracking of beaked whales with conventional seafloor hydrophone arrays in which receivers are spaced several kilometers apart, depth profiles of beaked whales recorded by time-synchronized suction-cup tags can be used to minimize the number of required receivers (Shaffer *et al.*, 2013). However, the difficulty of

[a]Electronic mail: mgassmann@ucsd.edu

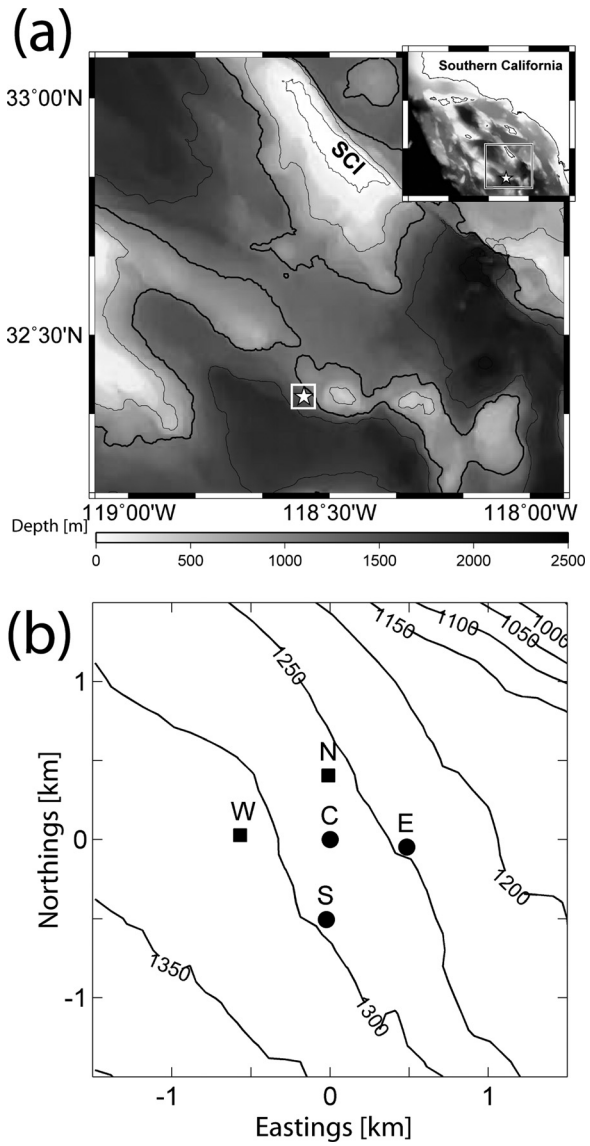

FIG. 1. (a) Location of the acoustic tracking array (star in the square box) in the Southern California Bight south of San Clemente Island (SCI). Black bathymetry contour lines are shown every 500 m. (b) Map of the seafloor array with five HARPs (C, N, E, S, and W) geo-referenced to HARP C (32° 22.194′ N 118° 33.774′ W). Circles and squares represent HARPs with one hydrophone or with a small-aperture array, respectively. High-resolution bathymetry was obtained from a multibeam SONAR scan on the R/V Revelle cruise CNTL05RR. Depths of contours are in meters below sea surface.

attaching tags limits the number of individuals that can be tracked with this approach. To understand beaked whales' behavior and behavioral responses to man-made sounds (DeRuiter *et al.*, 2013), horizontal movement patterns and their corresponding depth profiles from a large number of tracked individuals would be beneficial. Passive acoustic tracking has the potential to better facilitate whale behavior and movement pattern studies if the required number of widely spaced receivers for a three-dimensional localization can be reduced without relying on depth information from suction-cup tags or multipath arrivals. In this paper, we address the beaked whale localization problem by introducing two volumetric hydrophone arrays with element spacing of approximately 1 m (Wiggins *et al.*, 2012) into a conventional large-aperture seafloor array with a total of five nodes spaced up to 1 km apart. As a three-dimensional direction to an echolocating beaked whale can be estimated from each of the two small-aperture volumetric arrays, a three-dimensional location can be estimated by cross-fixing the two three-dimensional directions. This reduces the required number of widely spaced receivers to two for locations that are not collinear to the axis connecting the two volumetric arrays (Hirotsu *et al.*, 2010). To take advantage of the entire five node seafloor array, a maximum likelihood estimator is implemented that utilizes all available arrival times of an echolocation sound at the two volumetric arrays and the three single-hydrophone receivers to estimate the three-dimensional location of a Cuvier's beaked whale (*Ziphius cavirostris*). To illustrate the capabilities of this technique, single Cuvier's beaked whales, as well as groups of up to three individuals, were tracked within an area of 20 km^2 in the Southern California Bight with track durations up to 33 min. A total of 11 tracks provide insight into the behavior of deep-diving Cuvier's beaked whales such as elevation above the local seafloor in addition to source level estimates for echolocation and buzz sounds.

II. METHODS

A. Experimental setup

An array of five autonomous high-frequency acoustic recording packages (HARPs) with separations ranging from 406 to 1059 m was deployed on a seafloor slope in an area of known beaked whale habitat [site N in Baumann-Pickering *et al.* (2014) in the Southern California Bight (Fig. 1 and Table I)]. While the center (C), eastern (E), and southern (S) HARPs were each equipped with a single hydrophone (Wiggins and Hildebrand, 2007), the northern (N) and western (W) HARPs were each equipped with a volumetric array of four hydrophones (Wiggins *et al.*, 2012). The fixed array configuration was improved to reduce reflections from the support structure by mounting the four hydrophones at the top of fiber-glass masts. The hydrophone spacing ranged

TABLE I. Location and configuration of the HARPs. Latitude, longitude, and depth of redeployed HARPs E and S are given in parentheses.

HARP Site Name	Number of hydrophones	Sampling frequency [kHz]	Latitude [North]	Longitude [West]	Hydrophone depth [m]
C	1	200	32° 22.194′	118° 33.774′	1263
N	4	100	32° 22.414′	118° 33.781′	1256
E	1	200	32° 22.168 (32° 22.188′)	118° 33.464′ (118° 33.535′)	1227 (1235)
S	1	200	32° 21.922′ (32° 21.906′)	118° 33.789′ (118° 33.831′)	1277 (1282)
W	4	100	32° 22.209′	118° 34.137′	1310

from 0.9 to 1.7 m with the top hydrophone (#1) being 3.5 m above the seafloor [Figs. 2(a) and 2(b)]. For all HARPs, hydrophone sensitivities and transfer function calibrations were performed at the Scripps Whale Acoustics Laboratory and at the U.S. Navy's Transducer Evaluation Center facility in San Diego, California. Minima of the HARPs' peak-to-peak clipping levels ranged from 158.5 to 159.8 dB re 1 μPa at 42 kHz, which is close to the center frequency of Cuvier's beaked whale echolocation clicks.

Data were recorded continuously from December 2010 to February 2011 for 63 days at a sampling frequency of 200 kHz for the single sensor HARPs (C, E, and S) and at a sampling frequency of 100 kHz for the four-channel HARPs (N and W). On January 6, 2011, HARPs E and S were refurbished and redeployed 118 and 76 m westwards from their initial location, respectively.

To compute harmonic mean sound speeds (Send *et al.*, 1995) and to detect potential changes in the sound speed profile over the duration of the experiment, two full ocean depth conductivity, temperature, and depth (CTD) casts were conducted at the location of HARPs E and N during the seafloor array deployment and recovery, respectively. Figure 3 shows the seafloor-to-bottom CTD cast from the recovery day and the corresponding sound velocity profile (Del Grosso, 1974). No significant change in sound speed ($>1\,\mathrm{ms}^{-1}$) below depths of 35 m between deployment and recovery CTDs was found. From the deployment and recovery sound speed profiles, time-independent harmonic mean sound speeds of 1484.7 and 1484.9 ms^{-1}, respectively, were computed for steep surface-to-bottom paths.

The HARP locations (Table I) were estimated with a root-mean-square (rms) error of 4 m by applying a least-squares inverse to two-way travel times of pings travelling between a global positioning system (GPS)-located ship (R/V Sproul) and the acoustic release transponder of each HARP (Wiggins *et al.*, 2013). The known distances between the acoustic release transponders and the hydrophones (3 to 12.5 m) yield the hydrophone depth estimates in Table I. The time-invariant orientations of the static hydrophone arrays of HARPs N and W were obtained by cross-correlating the recorded broad-band ship noise from 150 GPS-referenced locations, which were horizontally distributed 360° around each HARP at a radius of less than the water depth, to minimize sound refraction effects caused by the depth-dependent sound speed profile. Using a spherical propagation model with a harmonic mean sound speed, c, for each ship location, $\boldsymbol{s_{i,j,k}} = (x_i,\ y_j,\ z_k)$, the predicted time-difference of arrival between two hydrophones p and q, with their location

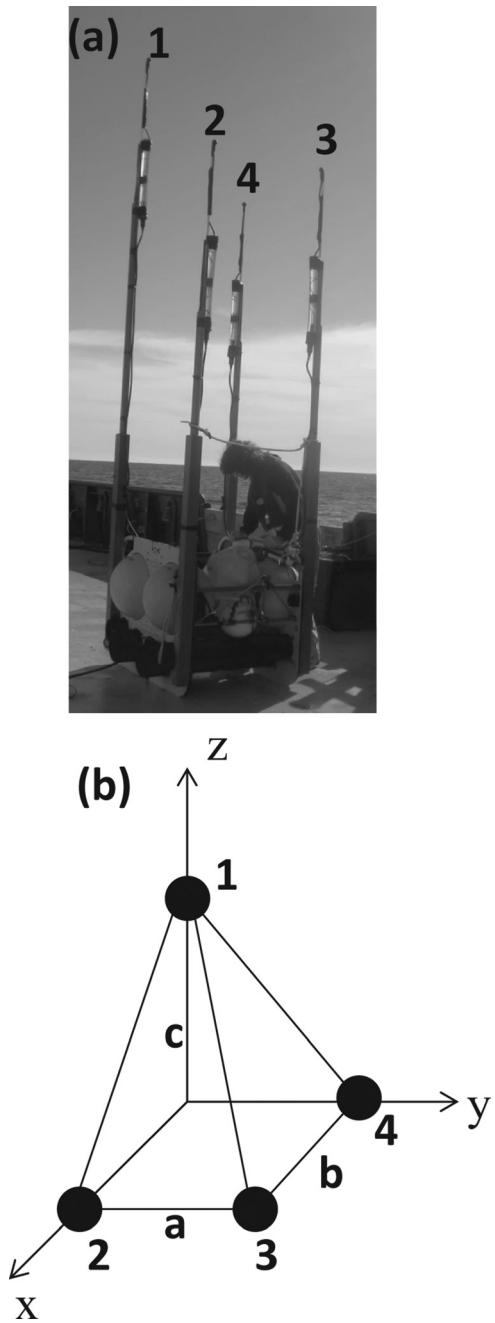

FIG. 2. (a) Small-aperture array of four hydrophones at the top of each vertical mast as indicated by the numbers 1–4, located above a HARP seafloor package. (b) Schematic of the small-aperture array configuration with its spacing a = 0.9 m, b = 1.1 m, and c = 0.9 m.

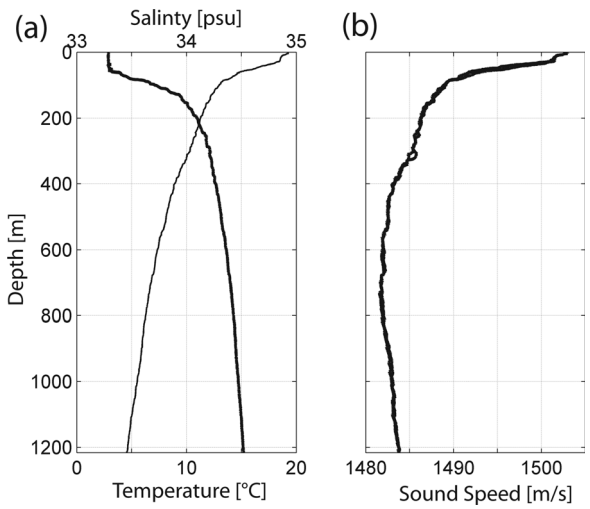

FIG. 3. (a) Salinity (thick line with upper horizontal scale) and temperature (thin line with lower horizontal scale) profile from surface-to-near seafloor, down and upward CTD cast near HARP N. (b) Estimated sound speed profiles according to (Del Grosso, 1974) based on temperature and salinity profiles from (a).

vectors $\boldsymbol{h_p} = (h_{px}, h_{py}, h_{pz})$ and $\boldsymbol{h_q} = (h_{qx}, h_{qy}, h_{qz})$, respectively, was obtained by

$$TDOA_{pred\ p,q} = \frac{\|\boldsymbol{h_p} - \boldsymbol{s_{i,j,k}}\| - \|\boldsymbol{h_q} - \boldsymbol{s_{i,j,k}}\|}{c}, \quad (1)$$

with $\|\cdot\|$ being the ℓ^2 norm, Eq. (1) yields a vector of the six predicted time-differences of arrival for each small-aperture array, $\boldsymbol{TDOA_{pred}}$. The sum of the squared differences between the predicted and cross-correlated time-differences of arrivals, $\boldsymbol{TDOA_{pred}}$ and $\boldsymbol{TDOA_{meas}}$, respectively, was minimized for all 150 ship locations to yield the hydrophone matrix, $\boldsymbol{H} = [\boldsymbol{h_1}, \boldsymbol{h_2}, \boldsymbol{h_3}, \boldsymbol{h_4}]$, which contains the Cartesian coordinates for each of the four hydrophones with respect to the geo-referenced acoustic transponder of each of the two HARPs with a small-aperture array,

$$\min\left\{\sum_i \sum_j \sum_k |\boldsymbol{TDOA_{pred}}[\boldsymbol{s_{i,j,k}}] - \boldsymbol{TDOA_{meas}}[\boldsymbol{s_{i,j,k}}]|^2\right\} \rightarrow \boldsymbol{H}. \quad (2)$$

According to the hydrophone matrices, $\boldsymbol{H}$, the x axis of HARPs N and W, as defined in Fig. 2(b), was orientated at a bearing of 210° and 312°, respectively. There was no significant inclination of the x-y plane relative to the sea surface for the small-aperture arrays at N and W. The small-aperture array orientations were confirmed by estimating three-dimensional directions (Wiggins *et al.*, 2012) to the three single-hydrophone HARPs (using their transponder reply pings), and to known ship GPS locations, with a rms error of less than 3°.

To ensure clock synchronicity between the five HARPs, pings from the HARPs' acoustic transponders were emitted and received at each known HARP location at the beginning, after 27 days and at the end of the experiment in addition to measuring drift rates and offsets before and after the deployments with a high precision (100 ns) satellite-based clock (Wiggins *et al.*, 2013). HARP clock drift rates were constant over the duration of the deployment, but varied across the HARPs between 8.8×10^{-10} (HARP C) and 2.8×10^{-9} (HARP N). This results in a total drift of 4.8 ms for HARP C and 15.2 ms for HARP N over the deployment of 63 days.

B. Acoustic detection and classification of Cuvier's beaked whale sounds

During their dives, Cuvier's beaked whales produce regular echolocation sounds, called clicks. The unique features of Cuvier's beaked whale click signals, throughout the world's oceans and in particular in the Southern California Bight, have been previously described and hence enable unambiguous classification of this species (Baumann-Pickering *et al.*, 2014). While start and end times of Cuvier's beaked whale dives were manually determined in long-term spectrograms of the acoustic data (Wiggins and Hildebrand, 2007), a Teager energy detector was used to detect the clicks automatically on each of the five HARPs (Roch *et al.*, 2011). In addition to clicks, we observed other sounds such as rapid click trains, called buzzes (Johnson *et al.*, 2004). If a localized buzz sound originates from near a Cuvier's beaked whale regular-click location and no other marine mammal species was acoustically present, it was considered with high confidence that the buzz was emitted by the regular-click localized Cuvier's beaked whale.

C. Three-dimensional localization

1. Click association and time-difference of arrival computation

Each detected click on any given HARP was associated with the clicks detected on the other four HARPs within a given time window to exclude click associations that exceed the maximum possible TDOAs between the five HARPs. The maximum possible TDOA for each of the 10 large-aperture hydrophone pair combinations ranged from 0.274 to 0.714 s and was computed as the quotient of the slant ranges between any two HARPs and the near-seafloor sound speed. Hence, the time windows for the four peripheral HARPs were centered at the click arrival time of the center reference HARP and had a maximum duration of the click duration plus two times the maximum possible time lag between the two HARPs on which the clicks were detected.

Ambiguous click associations can exist for groups of clicking beaked whales and for HARP pairs with maximum possible TDOAs greater than the beaked whales' inter-click-interval (ICI), especially since most clicks were not recorded by all five HARPs due to the echolocation click's beam directionality with a directivity index (DI) of 25 dB as estimated by Zimmer *et al.* (2005). Therefore, the TDOA of the associated clicks were computed and displayed for each HARP pair for an entire dive, yielding semi-continuous TDOA trajectories from which the ambiguities can be manually resolved. In contrast to the large-aperture array, no ambiguities in click associations for the small-aperture arrays needed to be resolved since a click was always received on all four hydrophones and the maximum possible TDOA was on the order of 1 ms.

TDOAs were computed from the peak of the cross-correlated times series between pairs of hydrophones. The total number of TDOAs depends on the number of HARPs that received a given click and ranged from 15 to 22 TDOAs. For instance, when a click is received on all five HARPs, 22 TDOAs were used: 6 TDOAs from each of small-aperture arrays, gathered in the vector $\boldsymbol{TDOA_{smlmeas}}$ and 10 TDOAs from the five-element large-aperture array (only hydrophone #1 is used from HARP N and W), gathered in the vector $\boldsymbol{TDOA_{lrgmeas}}$. We required that clicks were received on three or more HARPs and that small-aperture array HARPs were included in the solution, with 15 being the minimum number of TDOAs required for estimating a three-dimensional location.

2. Grid search algorithm

To find the location of the click-emitting beaked whale in Cartesian coordinates, $\boldsymbol{s_{Zc}} = (x_{Zc}, y_{Zc}, z_{Zc})$, a maximum likelihood estimator (Nosal and Frazer, 2007) was

implemented that minimizes the sum of the squared differences of the measured ($\boldsymbol{TDOA_{smlmeas}}$ and $\boldsymbol{TDOA_{lrgmeas}}$) and the predicted ($\boldsymbol{TDOA_{smlpred}}$ and $\boldsymbol{TDOA_{lrgpred}}$) sets of time-differences of arrivals for the small and large-aperture arrays, for each source location candidate, $\boldsymbol{g_{i,j,k}} = (x_i, y_j, z_k)$, within the defined model space.

To compute the predicted $\boldsymbol{TDOA_{smlpred}}$ $(\boldsymbol{g_{i,j,k}})$ and $\boldsymbol{TDOA_{lrgpred}}$ $(\boldsymbol{g_{i,j,k}})$ at each grid point, $\boldsymbol{g_{i,j,k}}$, a spherical propagation model [Eq. (1)] with a constant sound speed of $c = 1484\,\mathrm{ms}^{-1}$ was used due to negligible sound refraction effects for rays launched to the HARPs between 600 m depth and the seafloor [$< 2\,\mathrm{ms}^{-1}$ change in sound speed according to Fig. 3(b)]. The source location candidates, $\boldsymbol{g_{i,j,k}}$, were distributed horizontally ± 5 km and vertically from 300 to 1500 m depth with respect to the geo-referenced HARP C hydrophone to cover all potentially detectable Cuvier's beaked whale locations. For computational considerations, the horizontal and vertical resolution was initially 100 m to provide an overall sense of the beaked whale trajectories. Based on the initial results, the horizontal and vertical limits on the source location candidates were decreased, and the vertical and horizontal resolution was increased to 10 m (smaller than two times the length of a Cuvier's beaked whale).

To account for orders of magnitudes discrepancy between the small and large-aperture TDOAs, two likelihood surfaces, one for the small-aperture arrays, L_{sml}, and one for the large-aperture arrays, L_{lrg}, were defined. For each location candidate, $\boldsymbol{g_{i,j,k}}$, within the defined model space, the value of L_{sml} and L_{lrg} is computed, respectively, by

$$L_{sml}(\boldsymbol{g_{i,j,k}}) = \left(2\pi\sigma_{sml}^2\right)^{-N/2} \exp\left(\frac{-1}{2\sigma_{sml}^2}\sum_{n=1}^{N}\left|TDOA_{smlmeas_n}[\boldsymbol{s_{Z_c}}] - TDOA_{smlpred_n}[\boldsymbol{g_{i,j,k}}]\right|^2\right), \tag{3}$$

$$L_{lrg}(\boldsymbol{g_{i,j,k}}) = \left(2\pi\sigma_{lrg}^2\right)^{-M/2} \exp\left(\frac{-1}{2\sigma_{lrg}^2}\sum_{m=1}^{M}\left|TDOA_{lrgmeas_m}[\boldsymbol{s_{Z_c}}] - TDOA_{lrgpred_m}[\boldsymbol{g_{i,j,k}}]\right|^2\right), \tag{4}$$

where M represent the number of the measured large-aperture TDOAs with a maximum value of 10 for a click received on all five HARPs, and N equals the number of the measured small-aperture TDOA and is either 6 or 12 for a click received on one or two small-aperture arrays, respectively.

The standard deviations σ_{sml} and σ_{lrg} scale L_{sml} and L_{lrg} while accounting for the aperture-dependent uncertainties in hydrophone locations and cross-correlation derived TDOA measurements

$$\sigma_{sml} = \sqrt{\sigma_{H_{sml}}^2 + \sigma_{xcorr_{sml}}^2}, \tag{5}$$

$$\sigma_{lrg} = \sqrt{\sigma_{H_{lrg}}^2 + \sigma_{xcorr_{lrg}}^2}, \tag{6}$$

with $\sigma_{H_{sml}} = 0.1 \times 10^{-3}$ s and $\sigma_{xcorr_{sml}} = 0.05 \times 10^{-3}$ s for the small-aperture array and $\sigma_{H_{lrg}} = 5 \times 10^{-3}$ s and $\sigma_{xcorr_{lrg}} = 0.3 \times 10^{-3}$ s for the large aperture array.

The source location, $\boldsymbol{s_{Zc}}$, is found by maximizing the combined likelihood surface, L. For each location candidate, $\boldsymbol{g_{i,j,k}}$, the value of L is computed by

$$L(\boldsymbol{g_{i,j,k}}) = L_{sml}(\boldsymbol{g_{i,j,k}}) L_{lrg}(\boldsymbol{g_{i,j,k}}). \tag{7}$$

Error estimates for a computed source location, $\boldsymbol{s_{Zc}}$, can be obtained from the 95% confidence intervals of the combined likelihood surface, L, for each of the three spatial dimensions (Nosal and Frazer, 2007). For example, to estimate the error of x_{Zc}, the y and z values are kept fixed at the values of the estimated source location, y_{Zc} and z_{Zc}, to yield a conditional likelihood function (CLF), $L(x|y = y_{Zc}, Z = z_{Zc})$. To identify the 95% confidence interval, a discrete cumulative CLF, $C(x)$, is computed,

$$C(x) = \sum_{x_i < x} L(x_i | y = y_{Zc}, z = z_{Zc}). \tag{8}$$

$C(x)$ is normalized by its maximum value so that its values range between 0 and 1. The lower and upper limits of the 95% confidence interval of x_{Zc} are found by the x values that satisfy best $C(x_{2.5\%}) = 0.025$ and $C(x_{97.5\%}) = 0.975$, respectively, for the grid resolution of 10 m (Nosal and Frazer, 2007). For y_{Zc} and z_{Zc}, the 95% confidence intervals are obtained in the same fashion.

The 95% confidence intervals depend non-linearly on the source locations with respect to the HARP array and the number of HARPs that received the clicks. For horizontal locations inside the array and elevations of up to 300 m above the array, the 95% confidence intervals typically vary between 20–50 m horizontally and between 30–80 m vertically. For locations outside the array, but within 2 km horizontal and 800 m vertical radius, the horizontal and vertical location errors typically range between 40–70 m and 60–140 m, respectively.

D. Source time series and source levels

To account adequately for differences in the attenuation coefficient across a click's frequency bandwidth (> 5 dB/km between 30 and 50 kHz in Fig. 4), source levels were

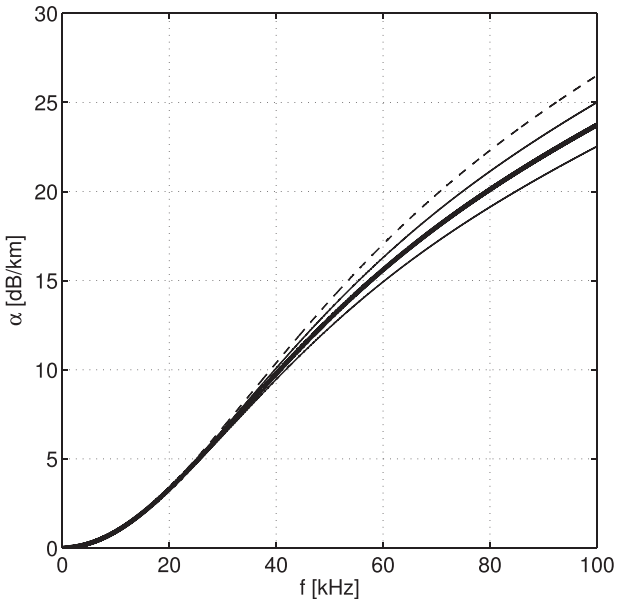

FIG. 4. Sound absorption coefficient α as a function of frequency (Ainslie and McColm, 1998) at the HARP array based on the CTD data shown in Fig. 3(a) for a pH of 7.3. Thick line represents α at 1000 m and is used in Eq. (9). Depth, temperature and salinity dependence of α is illustrated by the lower solid, upper solid, and dashed line for the CTD data at 1200, 800, and 600 m depth, respectively.

estimated from source pressure time series in contrast to computing an apparent source level from the received pressure time series with an averaged, fixed attenuation coefficient (e.g., Zimmer *et al.*, 2005; Shaffer *et al.*, 2013).

The source pressure time series of a click at a reference distance of 1 m, $s(t)$, is obtained by propagating the calibrated received pressure time series from the hydrophone along the computed slant range, r, in meters, back to the beaked whale, using a spherical propagation model and the frequency-dependent attenuation coefficient, $\alpha(f)$, in dB/km, with $\omega = 2\pi f$,

$$s(t) = \frac{r/1m}{2\pi}\int_{-\infty}^{+\infty} X(\omega)G(\omega)H(\omega)e^{k\alpha(\omega)r}e^{i\omega t}d\omega. \quad (9)$$

In Eq. (9), $X(\omega)$ is the Fourier transform of the received acoustic pressure time series $x(t)$,

$$X(\omega) = \int_{-\infty}^{+\infty} x(t)e^{-i\omega t}dt. \quad (10)$$

The inverse Fourier and Fourier transforms of Eqs. (9) and (10) were computationally implemented using a fast Fourier transform (FFT) algorithm.

$G(\omega)$ represents the inverse hydrophone-specific transfer function obtained from calibrations that were performed at the Scripps Whale Acoustics Laboratory and at the U.S. Navy's Transducer Evaluation Center facility in San Diego, CA. $H(\omega)$ is a digital band-pass filter of order 64, which selects the frequency bands of $X(\omega)$ that are greater than 15 kHz and above the noise floor to retain only signal components introduced by beaked whales. The noise floor between 15 and 100 kHz is computed before each click and determines the number of the stop and pass bands with their corresponding cutoff frequencies for each received click individually. Power spectral density (PSD) levels of the noise floor were below 52 dB re 1 μPa^2/Hz for all HARPs.

The constant k equals $[2 * 10^4 * \log(e)]^{-1}$ and is required in Eq. (9) to convert the attenuation coefficient $\alpha(\omega)$ from dB/km to Neper/m while the angular frequency dependence of $\alpha(\omega)$ maps to $\alpha(f)$ simply by $\omega = 2\pi f\alpha(f)$. $\alpha(f)$ was computed (Ainslie and McColm, 1998) for the depth (1000 m) near which most of the Cuvier's beaked whale clicks were localized using a temperature of 4.1 °C and a salinity of 34.47 psu (practical salinity units) as measured by the two CTD casts. A pH of 7.3 was used, based on pH measurements up to 1100 m depth about 27 km west and east of the hydrophone array in 2013 [CLIVAR & Hydrographic Data Office; http://cchdo.ucsd.edu/cruise/318M20130321 (last viewed June 25, 2015)]. Variations of the attenuation coefficient due to changes in salinity, temperature and pH in the depth layer in which more than 95% of all beaked whales were localized (800–1200 m) are negligible below 50 kHz and less than ± 1 dB/km around 70 kHz (Fig. 4).

Estimated directly from the computed source pressure time series, $s(t)$, of Eq. (9) were (1) the peak to peak source level, SL_{pp}, (2) the total energy flux based on the 97% energy criteria, E_{97}, and in addition, (3) the rms source level based on the 97% energy criteria, SL_{rms97}, to be consistent with the metrics used in previous literature for Cuvier's beaked whales and similar species (Zimmer *et al.*, 2005; Shaffer *et al.*, 2013). For calculating E_{97}, an average acoustic impedance (1,531,500 Rayl) was estimated from the CTD data for the water layer between 600 and 1200 m depth (Millero *et al.*, 1980).

For the received and computed source pressure time series, calibrated energy spectral densities (ESD) in dB re 1 μPa^{2}s/Hz of the clicks were computed, to avoid issues raised for PSD levels of transient sounds (Madsen, 2005). Note that the EDS levels differ from PSD levels by $10\log(T_S)$, where T_S is the signal length.

E. Click directionality

To investigate the directionality of Cuvier's beaked whale clicks, each SL_{pp} of a click can be associated with an angle that is measured between the acoustic axis of the whales' click sound beam, and the vector connecting the whale with the HARP from which the SL_{pp} was estimated. This angle will be referred to as the off-axis angle, γ, and ranges from 0° (looking forward along the acoustic axis) over 90° (perpendicular to the acoustic axis) to 180° (looking backward along the acoustic axis). Assuming that the acoustic axis of the whale's click beam was parallel to the whale's velocity vector during clicking, off-axis angles of clicks received at the HARPs with 100 kHz bandwidth (HARPs N, E, and S) were obtained by

$$\gamma = \sqrt{(\alpha')^2 + (\phi')^2}, \quad (11)$$

with

$$\alpha' = \tan^{-1}\left(\frac{b'_y}{b'_x}\right) \quad (12)$$

and

$$\phi' = \tan^{-1}\left(\frac{b'_z}{\sqrt{(b'_y)^2 + (b'_x)^2}}\right). \quad (13)$$

b'_x, b'_y, and b'_z are the components of the whale frame direction vector, $\boldsymbol{b}'$, and were computed according to Eqs. (9) and (16) in Nosal and Frazer (2007). Due to the insensitivity of γ to the whale's rotation around its acoustic axis, the matrix accounting for the whale's roll movements in Eq. (9) in Nosal and Frazer (2007) was omitted. The required time-varying velocity vector, $\boldsymbol{v}(t) = (v_x(t),\ v_y(t),\ v_z(t))$, was smoothed by computing the first derivative of the $x(t)$, $y(t)$, and $z(t)$ component of the Cuvier's beaked whale track $\boldsymbol{s}_{Zc}(t)$ over a sliding time window of 20 s using linear regression.

For comparison, the broadband beam pattern of a flat circular piston model with a diameter of 0.5 m was implemented according to Eqs. (4)–(6) in Zimmer *et al.* (2005). For the Gaussian frequency weighting function in Eq. (9) in Zimmer *et al.* (2005), a center frequency of 42.1 kHz and a bandwidth of 7.9 kHz were used. The DI of the piston model was computed according to Eq. (7) in Zimmer *et al.* (2005).

III. RESULTS

Using the method described above, Cuvier's beaked whales were tracked within approximately 2.5 km with respect to the center of the hydrophone array at HARP C. A total of 11 tracks of Cuvier's beaked whales are shown in Fig. 5. These tracks include two encounters of single individuals [Figs. 5(a) and 5(b)], three encounters of two individuals [Figs. 5(c)–5(e)] and one encounter of three individuals [Fig. 5(f)]. The individual tracks will be referred to as a combination of the subplot number and, if multiple individuals are present, the track color. For example, the green track in subplot (c) of Fig. 5 will be referred to as 5(c) green.

Based on multiple-individual encounters [Figs. 5(c)–5(f)] individuals within the tracked groups are less than 1.5 km apart from each other during the encounter and are travelling, with respect to each other, in the same general direction with the exception of one Cuvier's beaked whale, which reversed its initial westward travel direction [5(c) green]. Another example of a beaked whale reversing its direction [5(b) from south to north between 22:19–22:24 GMT] occurred following its initial dive descent.

Buzzes were detected at the locations of the orange asterisks in Fig. 5(c) as two Cuvier's beaked whales approach each other (blue and green track) at a depth of 1240 m (elevation of 60 m above seafloor) and in Fig. 5(e) (blue track) at depth of 1090 m (elevation of 140 m above seafloor). The maximum peak to peak source level of the individual buzz clicks from each of the two buzz sounds were estimated from HARP N is 177 dB re 1 μPa @ 1 m and 179 dB re 1 μPa @ 1 m, respectively. The minimum ICI of the buzzes were 5.6 ms [Fig. 5(c)] and 7.3 ms [Fig. 5(e)].

The maximum duration and length of the tracks were 33 min [5(e) blue] and 2.9 km [5(d) blue], respectively. The average horizontal movement speed of each of the 11 tracks varies between 1 and 3 ms^{-1}. Foraging elevation varies greatly during and between the 11 individual tracks from seafloor depth to 400 m above the local seafloor.

A. Dive behavior and varying inter-click-interval

Dive and clicking behavior results are exemplified by the track of the Cuvier's beaked whale 5(b). The depth profile and the corresponding ICI as a function of time for this track are shown in Figs. 6(a) and 6(b), respectively. Over a period of 4 min, the single individual descends from about 500 to 1000 m depth, halting the descent at about 300 m above the local seafloor. During this period, the whale alternates between two ICI regimes as it reduces the time interval between clicks from about 0.6 to 0.3 s for one regime and from 0.9 to 0.55 s for the other regime [Fig. 6(b)]. At any given time, the two ICI rates are not related by a simple multiple, suggesting that a single interval with occasional skipping of clicks does not explain the timing.

Instead, it appears that the whale is purposely altering the ICI during its descent, both by gradually increasing the overall rate of clicking, and by alternating between a faster and slower clicking regime.

After 22:24 GMT, the Cuvier's beaked whale gradually ascends and descends three times (minimum of 875 m and maximum of 1050 m) as it moves north and westwards over a gently sloping bottom [Figs. 5(b) and 6(a)]. During this, presumably, foraging part of the dive, the ICI of Fig. 5(b) oscillates around a median of 497 ms, but has short-term patterns of ICI variation, as well as several gaps in clicking of several second duration.

The tracks of 5(d) green and 5(e) blue also contain a descent accompanied by two similar alternating and decreasing ICI regimes, followed by oscillations around a median ICI of approximately 500 ms during the foraging part of the dive. The other nine tracks show similar ICI oscillations, but contain neither a descent part nor two alternating and decreasing ICI regimes, presumably because these portions of the dive were beyond the range of the array where tracking was possible.

B. Click directionality

The beam pattern of the echolocation clicks, coupled with changes in direction of the animals, resulted in large changes in received signal levels and subsequent non-beam angle corrected (NBAC) source level estimates, as illustrated for track 5(b) in Fig. 7. The click peak-to-peak NBAC source levels of 5(b) varied between 160 and 224 dB re 1 μPa @ 1 m as estimated from HARPs N, E, and S [Figs. 7(a)–7(c)]. The remainder of this section relates the variations of the click peak-to-peak NBAC source levels of 5(b) to its three-dimensional track and concludes with a quantitative description of its directionality.

During the descent of 5(b) towards the ocean floor approximately 1.5 km south of the center of the HARP array, it is apparent that its echolocation beam sweeps twice over the HARP array within the first few minutes causing the SL_{pp} to rise twice up to about 215 dB re 1 μPa @ 1 m [Fig. 7(c)] and to drop below 195 dB re 1 μPa @ 1 m in between [Figs. 7(a)–7(c)]. As 5(b) transitioned from the descent to the foraging part of the dive at 22:23 GMT, no clicks were detected on

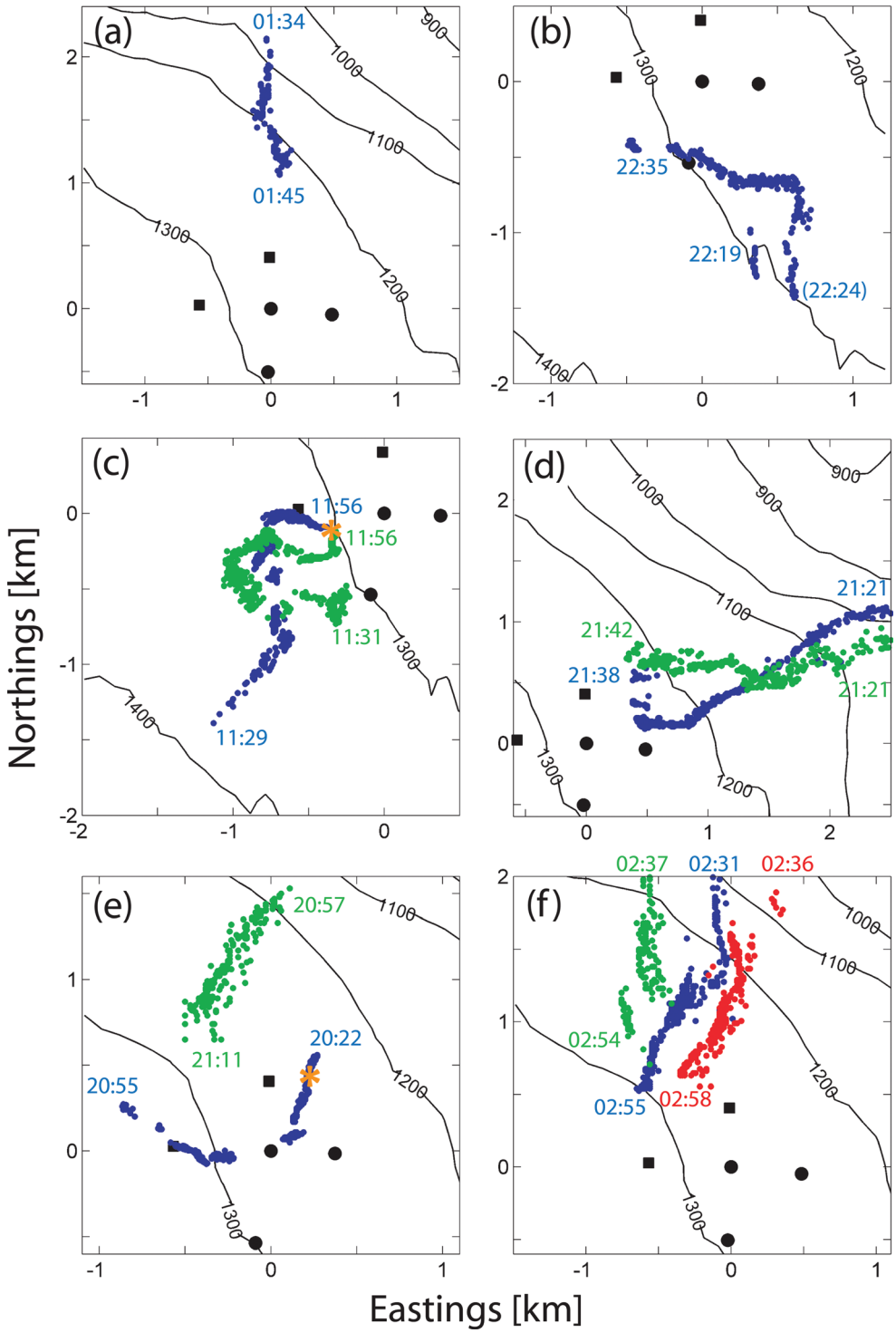

FIG. 5. Six maps of 11 tracks of Cuvier's beaked whales (color dots) with respect to the HARP array (black squares and circles) showing two singles (a) and (b), three groups of two individuals (c)–(e), and one group of three individuals (f). Blue, green, and red color of dots distinguishes between different individuals within a group. Locations of buzzes are indicated by orange asterisks in (c) and (e). Start and end times of each track are shown in GMT in hh:mm format for December 29, 2010 (a), February 7, 2011 (b), January 7, 2011 (c), December 19, 2010 (d), January 9, 2011 (e) and December 29, 2010 (f). Time in parentheses in (b) indicates transition between descending and foraging part of dive. Black contour lines represent water depth in meters. (b), (c), and (e) show HARP array with the locations of the redeployed HARPs E and S.

any of the five HARPs for 45 s. However, when 5(b) started the foraging part of its dive northwards towards the HARP array shortly after 22:24 GMT, the SL_{pp} increased rapidly to 224 dB re 1 μPa @ 1 m on HARP E [Fig. 7(b)], which is a source level 10 dB higher than previously reported for Cuvier's beaked whales (Zimmer *et al.*, 2005).

As 5(b) approached the HARP array horizontally by traveling northwards [Fig. 5(b)], but simultaneously ascended by approximately 200 m [Fig. 6(a)], the SL_{pp} decreases on HARPs N, E, and S by more than 20 dB (Fig. 7). This trend is reversed rapidly on HARPs N and E as 5(b) turned sharply westward and started to descend towards the

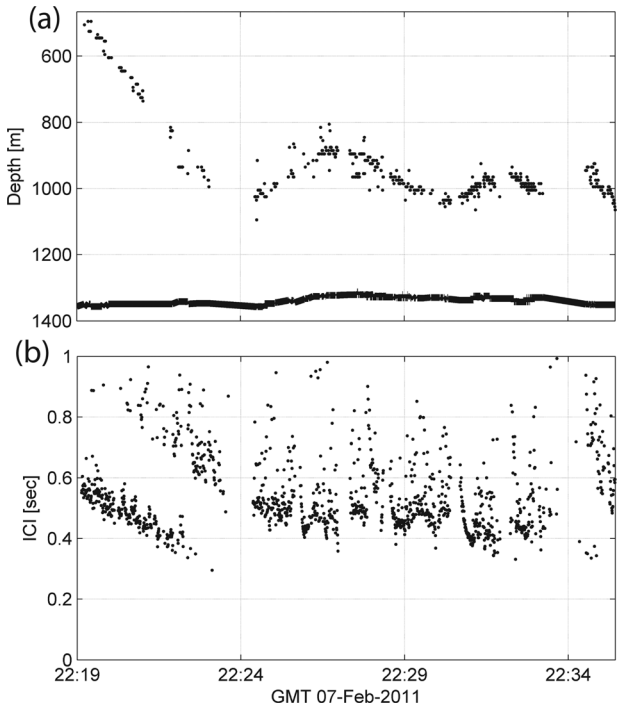

FIG. 6. (a) Depth profile of Cuvier's beaked whale track shown in Fig. 5(b). Local seafloor is indicated by the thick black line. (b) Corresponding ICI of clicks recorded on HARP N.

HARPs around 22:27 GMT. During this maneuver, it emitted a click towards HARP N with a SL_{pp} of 222 dB re 1 μPa @ 1 m as its beam moved counter-clockwise through the array from HARP E over N to S.

During the final portion of the track, 5 b finished its turn and headed westward, the SL_{pp} on HARP S increased dramatically by more than 20 dB until 22:29 GMT while the SL_{pp} decreased simultaneously on HARPs N and E. After 22:29 GMT, 5(b) started to head northwest and to ascend, which coincided with a dramatic decrease of SL_{pp} to 160 dB re 1 μPa @ 1 m on HARP S compared to a moderate decrease of SL_{pp} on HARPs N and E to 172 dB re 1 μPa @ 1 m despite the close horizontal proximity of 5(b) to HARP S [Figs. 5(b), 6(a) and 7]. As 5(b) descended towards the seafloor around 22:33 GMT, the SL_{pp} on HARP S increased strongly to SL_{pp} of 180 dB re 1 μPa @ 1 m, which is similar to HARPs N and E.

To quantitatively characterize the directionality of the echolocating Cuvier's beaked whale 5(b), the SL_{pp} estimates from HARPs N, E, and S (total of 2055 estimates), as shown in Figs. 7(a)–7(c), were plotted against their off-axis angles as blue, green, and red dots, respectively (Fig. 8). The ten clicks with the highest SL_{pp} between 210 and 224 dB re 1 μPa @ 1 m define the peak of the $SL_{pp}(\gamma)$ distribution at off-axis angles in the vicinity of 30°, which reveals the actual acoustic axis of the click's sound beam. Hence, such clicks will be referred to as either on-axis or near on-axis clicks depending on their SL_{pp} and their near-alignment to estimated axis of the whales' sound beam. For off-axis angles smaller or greater than 30°, the $SL_{pp}(\gamma)$ distribution decreases dramatically by several tenths of dB despite its high variations (>10 dB). A radial broadband piston beam

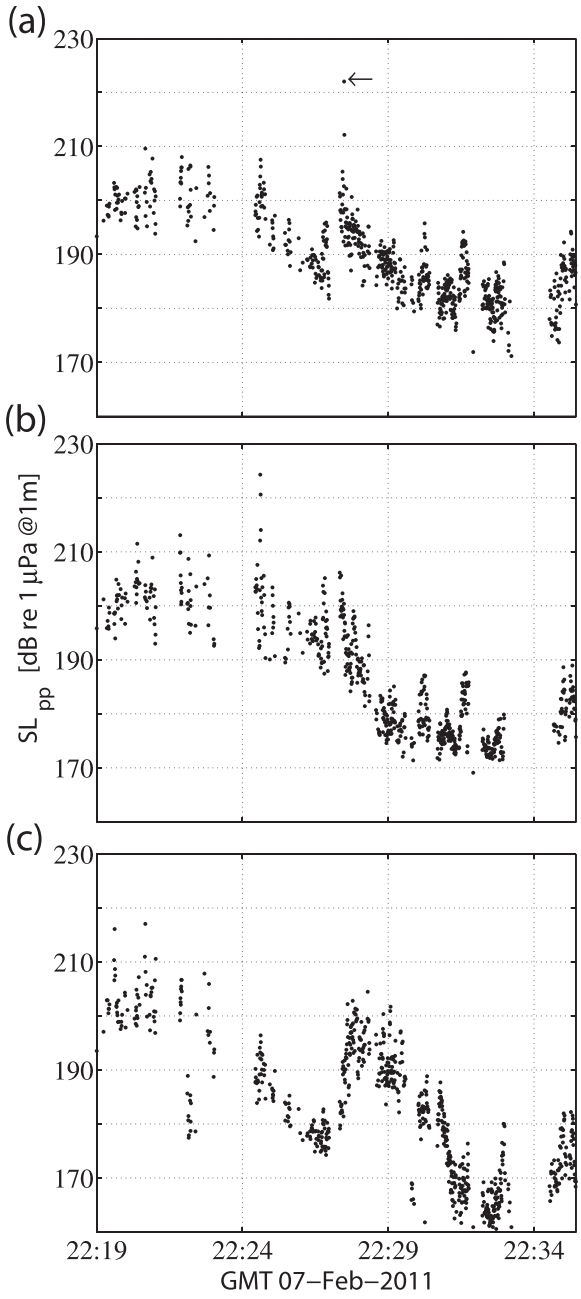

FIG. 7. Peak to peak source level estimates (SL_{pp}) of clicks recorded on HARPs N (a), E (b), and S (c) for the track in Figs. 5(b) and 6. Leftward arrow in (a) highlights the on-axis click discussed in Sec. III C.

pattern (black line in Fig. 8) was fitted to the $SL_{pp}(\gamma)$ distribution with a piston diameter of 0.5 m and a corresponding DI of 30 dB, which is within the DI range previously reported for Cuvier's beaked whales (Zimmer *et al.*, 2005).

C. Energy spectral density and high-frequency components

The on-axis click ($\gamma = 32°$) highlighted by a leftward arrow in Figs. 7(a) and 8 has a SL_{pp} of 222 dB re 1 μPa @ 1 m, a SL_{rms97} of 205 dB re 1 μPa @ 1 m and a total energy flux (E_{97}) of 172 dB re 1 μPa^2 s @ 1 m. Its spectral and temporal properties are shown in Fig. 9. The estimated energy spectral density (ESD) of the click at the reference distance of 1 m from 5(b) [blue line, Fig. 9(a)] shows that the majority of click

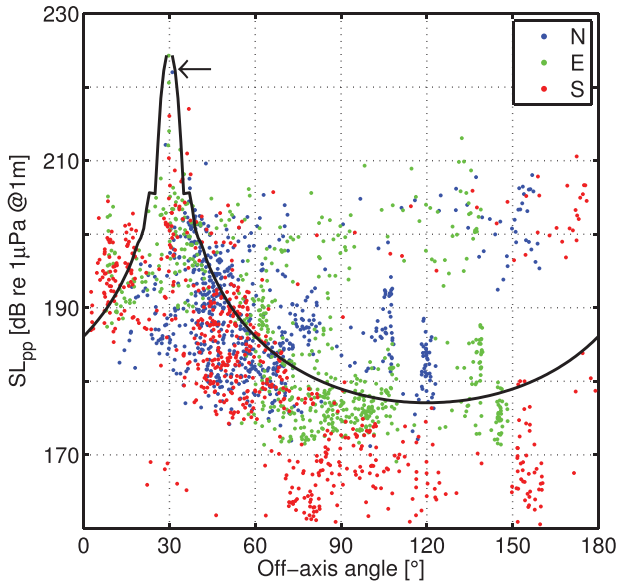

FIG. 8. Peak to peak source level estimates (SL_{pp}) of 2055 clicks as a function of off-axis angle for the track in Figs. 5(b) and 6. Clicks received by HARPs N, E, and S are represented by the blue, green, and red dots, respectively, and correspond to the clicks shown in Figs. 7(a)–7(c). Black line represents a piston model with a diameter of 0.5 m. Leftward arrow highlights the on-axis click discussed in Sec. III C.

energy is concentrated between 40 and 60 kHz with a side lobe at 23.3 kHz that is 23 dB lower than the maximum of the main lobe at 47.8 kHz. This spectral shape is consistent with what has been previously reported (Zimmer *et al.*, 2005). However, there are two additional high-frequency lobes at 72.2 and 91.1 kHz present in the source ESD estimated at 1 m that are, respectively, 6 and 9 dB lower than the maximum of the main lobe. Note, that for the ESD of the click received at HARP N at 1 km distance from 5(b), the two high-frequency lobes are 11 and 20 dB lower than the maximum of the main lobe at 58 dB re 1 μPa^2 s/Hz @ 1 km [solid green line in Fig. 9(a)], but well above the noise floor [green dotted line in Fig. 9(a)] by more than 10 dB. In addition, the 91.1 kHz lobe is 14 dB higher than the 23.3 kHz lobe in the source ESD at 1 m distance in contrast to the ESD received at 1 km distance, where the 91.1 kHz lobe is 4 dB lower than the 23.3 kHz lobe. This is due to the high absorption of sound in seawater at high frequencies in conjunction with the strong frequency dependence of the sound absorption over the bandwidth of the Cuvier's beaked whale click (3 dB/km at 20 kHz in contrast to 22 dB/km at 90 kHz as illustrated in Fig. 4).

The high frequency components of the click are present between 0.085 and 0.295 ms while the main lobe is a frequency-modulated upsweep that lasts until 0.4 ms as shown in the source pressure time series at 1 m and in the spectrogram [Figs. 9(b) and 9(c)]. Near on-axis clicks with frequency components above 60 kHz have also been observed for all of the other 10 Cuvier's beaked whale tracks at all HARPs sampling at 200 kHz (N, E, and S). However, the 90 kHz lobe is not present in the received ESD of these near on-axis clicks if the distance between the Cuvier's beaked whale and the recorder is greater than 1 km, such as for the near on-axis click emitted by 5(b) at 1.4 km distance from HARP N with an SL_{pp} of 224 dB re 1 μPa @ 1 m.

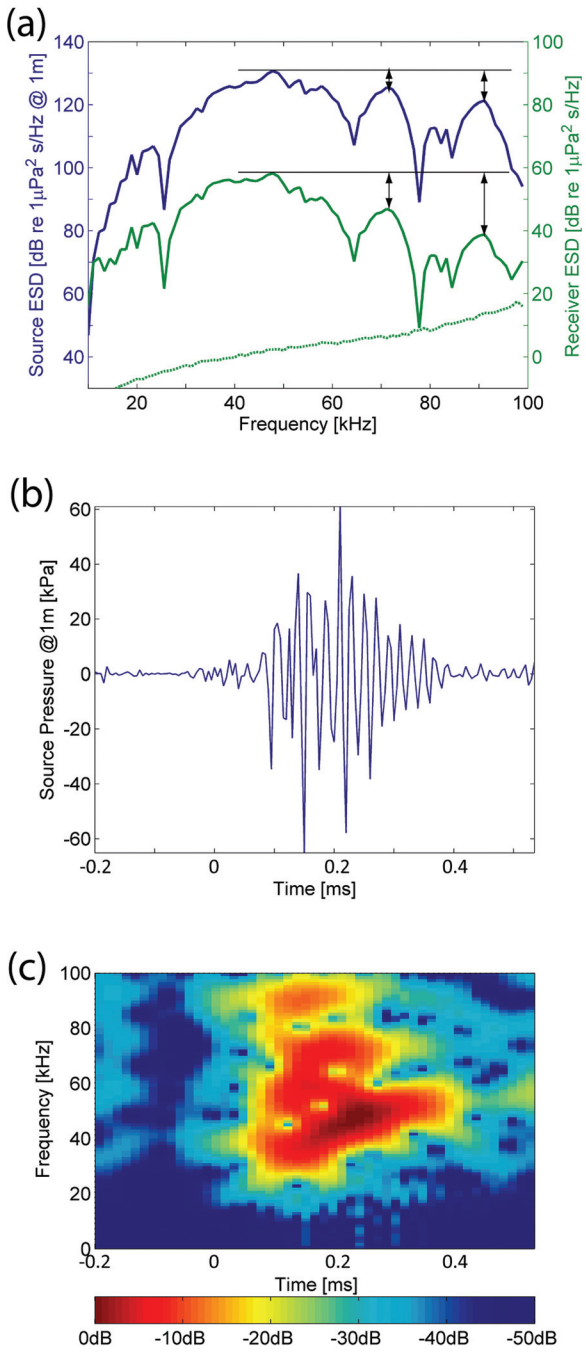

FIG. 9. On-axis beaked whale click: (a) Source (blue) and received (green) energy spectral density (ESD) along with equivalent noise floor (dotted green), (b) source pressure time series, and (c) normalized source spectrogram. Source ESD and pressure time series at a reference distance of 1 m were estimated for a click received by HARP N at a slant range of 1 km [click highlighted by leftward arrow in Figs. 7(a) and 8]. The Source ESD is referenced to the left vertical axis, whereas the received ESD and noise floor share the right vertical axis in (a). In addition to the frequency-modulated (FM) upsweep at 30–60 kHz, high-frequency (HF) components at 72 and 91 kHz in the source ESD were recovered from the received ESD by using Eq. (9). Whereas being greatly attenuated in the received ESD with respect to the maximum of the FM upsweep (lower set of vertical double arrows), the HF components are less than 9 dB below the maximum of the source ESD (upper set of vertical double arrows). Note that the noise floor is at least 10 dB below the received ESD, except for the vicinity of 78 kHz. The click's total energy flux is 172 dB re 1 μPa^2 706 s @ 1 m and its peak to peak source level is 222 dB re 1 μPa @ 1 m, estimated from the source pressure time series in (b). Source spectrogram in (c) was calculated with 32 sample FFTs with 90% overlap from the source pressure time series in (b) and normalized by its maximum.

IV. DISCUSSION

Uncertainties in the HARP locations, small-aperture array orientations, cross-correlation based TDOAs and time-synchronizations reduce the accuracy of the maximum likelihood estimator's click localization estimates, so only movement features greater than 10–20 m can be resolved within 1–3 km distance from the array. To resolve movements on finer scales, for example, to investigate foraging helical movements (Johnson *et al.*, 2004), advanced tracking or smoothing filters can be applied.

Although the localization method used here allows the use of an acoustic propagation model such as BELLHOP (Porter, 2005) instead of a spherical propagation model with a constant sound speed, there is no significant advantage in using a ray-trace model such as BELLHOP for deep-diving Cuviers' beaked whales below 500 m due to the negligible changes in sound speed at these depths. The difference in travel time of a ray obtained from a spherical propagation model with a constant sound speed of $1484\,\mathrm{ms}^{-1}$ versus BELLHOP with the depth-dependent sound speed profile is less than 1 ms for a 45 kHz source at 500 m depth at 2 km distance from a seafloor HARP. Given the uncertainties in the HARP location estimates of 4 m (equivalent to a travel time of approximately 3 ms using a sound speed of $1484\,\mathrm{ms}^{-1}$) and the limited accuracy of the eigenray-tracing capabilities of BELLHOP, we decided to use the spherical propagation model with a constant sound speed of $1484\,\mathrm{ms}^{-1}$. Even for the surface locations of the ship tracks that were used to calibrate the small-aperture array orientation, the difference in arrival angle of a straight path and the eigenray connecting the surface ship and a four-channel HARP is less than 0.07° at the four-channel HARP for ranges smaller than the water depth. This slope difference maps into a horizontal displacement of the surface ship of less than 25 m, which is less than the length of the ship (R/V Sproul) generating the sound. Furthermore, the high-resolution bathymetry data (obtained from the multibeam sonar survey during the R/V Revelle cruise CNTL05RR) needed to be adjusted to match the depths of the five HARPs to less than a few tens of meters.

Although information from tagged Cuvier's beaked whales suggests 30 buzzes per dive (Tyack *et al.*, 2006), only two buzz sound events were detected for the 11 Cuvier's beaked whale tracks. This low number may result from a lower detectability for buzzes due to lower source levels compared to clicks and also from different animal behavioral states that potentially could lead to fewer buzz sounds.

The use of alternating ICI regimes during the descent phase of the dive [Fig. 6(b)] warrants further examination. At 22:21 in Fig. 6, the animal is located at 600 m above the seafloor (740 m depth with 1340 m seafloor) and is using about 0.8 s for the long ICI regime; this delay is needed to wait for the seafloor echo to return before emitting another click. Likewise, at the end of the descent phase of the dive (22:23), the animal is about 340 m above the seafloor (1000 m depth with 1340 m seafloor) and using a 0.59 s long ICI, somewhat greater than what is needed for the seafloor echo to return. The short ICI regime, on the other hand, is consistently more rapid than the delay needed for the seafloor echo. This suggests that the animal may switch between these two regimes to both avoid ambiguity about the distance to the seafloor (long ICI regime) as well as to obtain closer echo information more rapidly (short ICI regime).

Despite frequent variations of over 40 dB, peak-to-peak source levels above 210 dB re 1 μPa @ 1 m are sparse for any given Cuvier's beaked whale track and for any of the five HARPs. This suggests that the acoustic axis of the Cuvier's beaked whale is rarely aligned with any of the seafloor HARPs. Uncertainty in the source level estimates are mainly driven by uncertainties in the localization with an upper limit of 3 dB and therefore, cannot explain the occasional presence of source levels up to 224 dB re 1 μPa @ 1 m. Although Eq. (9) recovers the magnitude of the high-frequency components of a click, these components do not contribute significantly to the peak-to-peak source level since the majority of the signal energy is contained in the frequency modulated upsweep between 40 and 60 kHz. Furthermore, the attenuation in sound intensity takes into account the sound absorption in seawater while ignoring scattering from inhomogeneities in the water such as prey items, since their distribution and properties are unknown. The increasing dependence of sound absorption on depth, temperature and conductivity with increasing frequency causes uncertainties of less than 0.5 to 1 dB/km for frequencies between 70 and 90 kHz in the energy spectral density estimate of a click (Fig. 4), but because of the relatively short ranges (< 2.5 km), these uncertainties are not significant. Despite small errors at higher frequencies, the remaining variations in the energy spectral densities of clicks are likely caused by natural variations in the Cuvier's beaked whale's click sound production and by the orientation of the acoustic axis of the Cuvier's beaked whale with respect to the hydrophone.

The large variations in the $SL_{pp}(\gamma)$ distribution are mainly driven by the uncertainties in the off-axis angle estimations rather than by the peak-to peak source level estimations (errors ≤ 3 dB as discussed above) if the natural variations in click directivity and peak-to-peak source level are assumed to be negligible. Uncertainties in the off-axis angles result from errors in estimating the whale's velocity vector and from its misalignment with the whales' acoustic axis during clicking due to head and yaw movements. The velocity vector is estimated as the first derivative of the linearly smoothed track 5(b) and hence, would benefit from applying more advanced tracking or smoothing filters to the track. This would not only help to reduce some of the variations in the $SL_{pp}(\gamma)$ distribution, but might also help to reduce the number of outliers (i.e., located between 90° and 180° at around 200 dB re 1 μPa @ 1 m in Fig. 8). The misalignment between the whale's acoustic axis and velocity vector could potentially also explain the presence of the $SL_{pp}(\gamma)$ distribution's peak at approximately 30°. In a previous, tag-based study of Cuvier's beaked whales, the $SL_{pp}(\gamma)$ distribution peaked at an off-axis angle between 18° and 35° (Zimmer *et al.*, 2005). In addition, the sound beam of echolocating Cuvier's beaked whales may be expected to not be aligned with the rostral axis of the marine mammal due to significant bilateral asymmetry (Cranford *et al.*, 2008). Hence, the 30° offset of the $SL_{pp}(\gamma)$ distribution's peak could

be, at least partly, caused by this phenomena, which remains subject to further investigation.

The high-frequency components above 60 kHz in Fig. 9 are unlikely to be harmonic distortions caused by non-linear effects of the analog recording chain between hydrophone and input of the analog-digital converter. Despite the high source levels of these clicks, their received levels are approximately 10 dB below the clipping levels of the HARPs and at these levels non-linear effects can be considered negligible.

V. CONCLUSIONS

By embedding volumetric small-aperture (~1 m element spacing) arrays into a large-aperture (~1 km element spacing) seafloor array, highly directional and deep-diving sound sources such as echolocating beaked whales can be tracked in all three spatial dimensions without relying on boundary reflections or depth information from suction-cup tags. The 11 Cuvier's beaked whale tracks presented here show movements of individuals as well as coordinated behavior within groups of up to three individuals over time periods from 10 to 33 min in an area of 20 km^2 around the center of the array. Beaked whale elevation above the seafloor varied during the foraging part of the dive by more than one hundred meters and between individuals from several tens of meters to several hundreds of meters. During the tracked descents of the dives, the Cuvier's beaked whales reduced gradually their ICI while alternating between two ICI regimes, apparently as means for tracking both their height above the seafloor and closer features.

For the localized echolocation clicks of one individual, peak-to-peak source levels of up to 224 dB re 1 μPa @ 1 m with a DI of 30 dB were estimated. The estimated source energy spectra at 1 m of the on-axis clicks show significant frequency components above the previously described FM upsweep. For buzz sounds, the maximum peak-to-peak source level was estimated to be 179 dB re 1 μPa @ 1 m. In addition, this passive acoustic tracking technique has the potential to collect large numbers of tracks over long periods to study three-dimensional movement patterns of deep-diving, echolocating odontectes without or with the presence of manmade noise.

ACKNOWLEDGMENTS

Funding for this research was provided by the U.S. Navy CNO-N45, the Naval Postgraduate School, Office of Naval Research, and the University of California ship fund program for young investigators. We thank Frank Stone, Ernie Young, Bob Gisiner, Curt Collins, John Joseph, Mike Weise, and Bruce Applegate for support and assistance. We also thank Mike Buckingham and Bill Hodgkiss for helpful discussion as well as the Scripps Whale Acoustics Lab members, especially Marie Roch and Simone Baumann-Pickering.

Ainslie, M., and McColm, J. (**1998**). "A simplified formula for viscous and chemical absorption in sea water," J. Acoust. Soc. Am. **103**, 1671–1672.

Baumann-Pickering, S., Roch, M. A., Brownell, Jr., R. L., Simonis, A. E., McDonald, M. A., Solsona-Berga, A., Oleson, E. M., Wiggins, S. M., and Hildebrand, J. A. (**2014**). "Spatio-temporal patterns of beaked whale echolocation signals in the North Pacific," PLoS One **9**, e86072.

Cranford, T. W., Mckenna, M. F., Soldevilla, M. S., Wiggins, S. M., Goldbogen, J. A., Shadwick, R. E., Krysl, P., Leger, J. A. S., and Hildebrand, J. A. (**2008**). "Anatomic geometry of sound transmission and reception in Cuvier's beaked whale (*Ziphius cavirostris*)," Anatom. Rec. **291**, 353–378.

Del Grosso, V. A. (**1974**). "New equation for the speed of sound in natural waters (with comparisons to other equations)," J. Acoust. Soc. Am. **56**, 1084–1091.

DeRuiter, S. L., Southall, B. L., Calambokidis, J., Zimmer, W. M., Sadykova, D., Falcone, E. A., Friedlaender, A. S., Joseph, J. E., Moretti, D., and Schorr, G. S. (**2013**). "First direct measurements of behavioural responses by Cuvier's beaked whales to mid-frequency active sonar," Biol. Lett. **9**, 20130223.

Gassmann, M., Elizabeth Henderson, E., Wiggins, S. M., Roch, M. A., and Hildebrand, J. A. (**2013**). "Offshore killer whale tracking using multiple hydrophone arrays," J. Acoust. Soc. Am. **134**, 3513–3521.

Hirotsu, R., Yanagisawa, M., Ura, T., Sakata, M., Sugimatsu, H., Kojima, J., and Bahl, R. (**2010**). "Localization of sperm whales in a group using clicks received at two separated short baseline arrays," J. Acoust. Soc. Am. **127**, 133–147.

Johnson, M., Madsen, P. T., Zimmer, W. M., De Soto, N. A., and Tyack, P. L. (**2004**). "Beaked whales echolocate on prey," Proc. R. Soc. London, Ser. B: Biol. Sci. **271**, S383–S386.

Madsen, R. T. (**2005**). "Marine mammals and noise: Problems with root mean square sound pressure levels for transients," J. Acoust. Soc. Am. **117**, 3952–3957.

Millero, F. J., Chen, C.-T., Bradshaw, A., and Schleicher, K. (**1980**). "A new high pressure equation of state for seawater," Deep Sea Res. Part A: Oceanogr. Res. Papers **27**, 255–264.

Nosal, E. M., and Frazer, L. N. (**2007**). "Sperm whale three-dimensional track, swim orientation, beam pattern, and click levels observed on bottom-mounted hydrophones," J. Acoust. Soc. Am. **122**, 1969.

Porter, M. (**2005**). "BELLHOP Gaussian beam/finite element beam code," Heat, Light, and Sound Research, Inc., http://oalib.hlsresearch.com/Rays/ (Last viewed 1/10/2015).

Roch, M. A., Klinck, H., Baumann-Pickering, S., Mellinger, D. K., Qui, S., Soldevilla, M. S., and Hildebrand, J. A. (**2011**). "Classification of echolocation clicks from odontocetes in the Southern California Bight," J. Acoust. Soc. Am. **129**, 467–475.

Schorr, G. S., Falcone, E. A., Moretti, D. J., and Andrews, R. D. (**2014**). "First long-term behavioral records from Cuvier's beaked whales (*Ziphius cavirostris*) reveal record-breaking dives," PLoS One **9**, e92633.

Send, U., Visbeck, M., and Krahmann, G. (**1995**). "Aspects of acoustic transponder surveys and acoustic navigation," in *Proceedings of OCEANs'95, MTS/IEEE, Challenges of Our Changing Global Environment*, Vol. 1633, pp. 1631–1642.

Shaffer, J. W., Moretti, D., Jarvis, S., Tyack, P., and Johnson, M. (**2013**). "Effective beam pattern of the Blainville's beaked whale (*Mesoplodon densirostris*) and implications for passive acoustic monitoring," J. Acoust. Soc. Am. **133**, 1770–1784.

Tiemann, C. O., Thode, A. M., Straley, J., O'Connell, V., and Folkert, K. (**2006**). "Three-dimensional localization of sperm whales using a single hydrophone," J. Acoust. Soc. Am. **120**, 2355.

Tyack, P. L., Johnson, M., Soto, N. A., Sturlese, A., and Madsen, P. T. (**2006**). "Extreme diving of beaked whales," J. Exp. Biol. **209**, 4238–4253.

Wiggins, S. M., Frasier, K. E., Henderson, E. E., and Hildebrand, J. A. (**2013**). "Tracking dolphin whistles using an autonomous acoustic recorder array," J. Acoust. Soc. Am. **133**, 3813–3818.

Wiggins, S. M., and Hildebrand, J. A. (**2007**). "High-frequency acoustic recording package (HARP) for broad-band, long-term marine mammal monitoring," in *International Symposium on Underwater Technology 2007 and International Workshop on Scientific Use of Submarine Cables & Related Technologies* (Institute of Electrical and Electronics Engineers, Tokyo, Japan), pp. 551–557.

Wiggins, S. M., McDonald, M. A., and Hildebrand, J. A. (**2012**). "Beaked whale and dolphin tracking using a multichannel autonomous acoustic recorder," J. Acoust. Soc. Am. **131**, 156–163.

Yack, T. M., Barlow, J., Calambokidis, J., Southall, B., and Coates, S. (**2013**). "Passive acoustic monitoring using a towed hydrophone array results in identification of a previously unknown beaked whale habitat," J. Acoust. Soc. Am. **134**, 2589–2595.

Zimmer, W. M. X. (**2013**). "Range estimation of cetaceans with compact volumetric arrays," J. Acoust. Soc. Am. **134**, 2610–2618.

Zimmer, W. M. X., Johnson, M. P., Madsen, P. T., and Tyack, P. L. (**2005**). "Echolocation clicks of free-ranging Cuvier's beaked whales (*Ziphius cavirostris*)," J. Acoust. Soc. Am. **117**, 3919–3927.